Experimental generation of broadband quadrature entanglement using laser pulses

Yun Zhang,* Tatsuya Furuta, Ryuhi Okubo, Kosuke Takahashi, and Takuya Hirano

Department of Physics, Gakushuin University, 1-5-1 Mejiro, Toshima-ku, Tokyo, 171-8588, Japan
CREST, Japan Science and Technology Agency, 1-9-9 Yaesu, Chuo-ku, Tokyo, 103-0028, Japan

We report on the generation of broadband pulsed quadrature entanglement by combining two squeezed vacua, which are generated from two degenerate optical parametric amplifiers (OPAs), on a beam splitter. With a single pass through OPA, in which a periodically poled lithium niobate waveguide is used as a nonlinear material, the noise reduction of 3.4 ± 0.2 dB below the shot noise limit is observed with a bandwidth of more than 200 MHz. The entanglement correlation or EPR correlation is confirmed with a sufficient criterion $\langle \Delta^2(X_a + X_b) \rangle + \langle \Delta^2(Y_a - Y_b) \rangle = 1.28 < 2$.

I. INTRODUCTION

Quantum entanglement or EPR correlation is one of the most fundamental properties of quantum mechanics and the most important resources in quantum communications and quantum information [1]. The originally devised quantum entanglement has been experimentally realized both in discrete variable and in continuous variable [2,3]. In the discrete variable regime, photon number are measured and pulse lasers are usually exploited as the light source. For each pulse, the photon number (one or zero) is measured by using a single photon detector and the quantum entanglement is examined relying on coincidence measurements. Meanwhile, in the continuous variable regime, a canonical conjugate variable called quadrature amplitude acts as the observable and continuous wave (cw) lasers usually are used as the light source. The quadrature amplitude of signal light are detected using a homodyne detector by interfering it with a local oscillator (LO) and the quantum entanglement is interrogated by measuring the quantum correlation between two beams. Thanks to a well-established quantum entanglement source, quantum information and communications have been rapidly developing in recent years and many quantum protocols, such as quantum teleportation [4], dense coding [5], or quantum cryptography, have been successfully implemented both in the discrete variable and in the continuous variable.

In practical communications protocol, it is very important to encode each relevant information on a carrier, which can be accessed individually. From this viewpoint, the laser pulses are the best candidate. Each laser pulse, which can be manipulated individually, can be utilized to encode one bit of individual information, furthermore the high repetition rate of pulse laser makes it possible to realize high-speed communication. Hence, an important issue for practical quantum information is to develop pulsed quantum entanglement state. To date many convincing experimental realizations of continuous-variable entanglement have been conducted based on different nonlinear effects in different media such as the second-order nonlinearity in optical parametric amplifier (OPA) either utilizing a nondegenerate optical parametric amplifier operating below it threshold [6–10] or a nondegenerate optical parametric oscillator (OPO) operating above it threshold [11,12] or two degenerate OPAs [4,13,14], and the third-order nonlinearity in atoms [15] or fibers [16,17]. Unfortunately, among the abovementioned experiments, there are few experiments on the realization of pulsed continuous-variable entanglement, particularly, using the laser pulses with high repetition rate. So, the realization of pulsed continuous-variable entanglement with high repetition rate still remains an experimental challenge.

In addition to the abovementioned potential for practical application, the pulsed continuous-variable entanglement has many other advantages in present quantum information science. First, it has a wide bandwidth in the frequency domain. It is well known that the wide bandwidth squeezing state can be generated by single pass OPA taking advantage of the high peak power of laser pulses [18,19]. Therefore, the combined entanglement by two squeezed states still keeps this property. Secondly, the experimental apparatus is simpler comparing with experiments using a cw laser as light source [20,21]. The high intensity during a pulse makes the build-up cavities, in which the intensity of light are enhanced so that nonlinear interaction is realized, and the cavity-lock servo system obsolete. Another advantage of pulsed nonclassical state is that it can be combined with measurement of another observable such as photon number besides quadrature observable for each pulse. Recently, Fock states of light with negative valued Wigner's quasiprobability distribution have been successfully observed using a conditional preparation scheme [22]. Fock state has been generated by a conditional measurement on quantum entanglement "twin" beams, which are produced by an OPA and contain perfectly correlated numbers of photons. Counting n photons in one mode projects the other mode in a n-photon state, which can then be analyzed using homodyne detection [23]. Furthermore single-photon added coherent states are also constructed using the abovementioned techniques [24]. On the other hand, "Schrödinger kitten" state and non-Gaussian state are also generated by photon subtracted squeezed vacuum states, where a small fraction of the squeezed state is split and detected by a photon counter as a trigger and the remaining signal beam is detected and analyzed using homodyne detector conditioned by the detected trigger photon [25,26].

―――――――
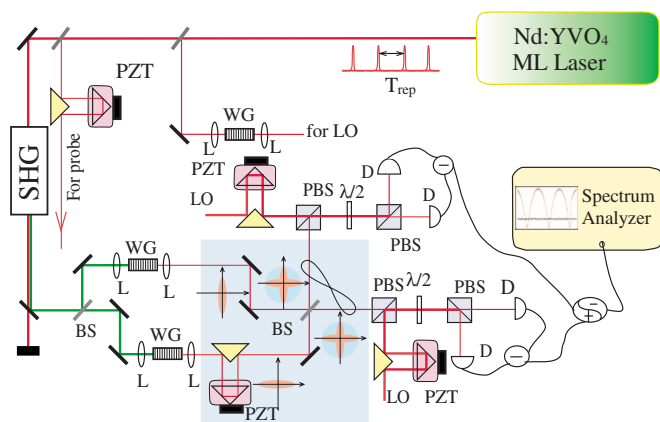*zhangyun@qo.phys.gakushuin.ac.jp

FIG. 1. (Color online) Experimental setup. SHG: second harmonic generator, WG: waveguide, BS: 50:50 beam splitter, L: lens, PBS: polarizing beam splitter, Ds: photodiodes, PZTs: piezoelectric transducers, λ/2: half-wave plate, and LO: local oscillator.

In this paper, we report on the generation of pulsed continuous variable quadrature entanglement by combining two squeezed vacua, which were generated by single pass OPA using single-mode periodically poled lithium niobate (PPLN) waveguide as a second-order nonlinear material, on a beam splitter. In contrast to most discrete-variable experiments involving laser pulses with high repetition rate, is the measurements of the quadrature amplitudes using a broad bandwidth homodyne detector. We observed squeezing of about 3.4 ± 0.2 dB below the shot noise limit over the bandwidth of 200 MHz. Thanks to good quality of PPLN waveguide, a -5.7 dB deamplification gain and more than 90% mode matching between the LO and probe in our experiment were obtained. By interference of two squeezed vacua, quantum correlation with about 3.2 dB below the shot noise level have been reached when one of a pair of entangled beams is measured. The entanglement correlation between two entangled beams is confirmed with a sufficient criterion $\langle \Delta^2(X_a + X_b) \rangle + \langle \Delta^2(Y_a - Y_b) \rangle = 1.28 < 2$ and we are able to achieve a reasonably faithful realization of the original pulsed entanglement in continuous variables with a high repetition rate laser pulses.

The paper is organized as follows. In Sec. II, we describe the experimental setup in detail with emphasis on a homodyne detection system with bandwidth of 200 MHz. In Sec. III, the technical details and results of the generation of broad bandwidth squeezing are discussed. Section IV is devoted to a description of the generation of pulsed entanglement state. Finally, we collect our conclusions in Sec. V.

II. EXPERIMENTAL CONFIGURATION

A. Experimental setup

The experimental scheme is presented in Fig. 1. The initial pulses are obtained from a cw mode-locked Nd:YVO$_4$ (VAN) laser, which is pumped by a semiconductor laser diode, operating at 1064 nm with a duration of 7 ps and a pulse repetition rate of 76 MHz. This laser system provided an average power of about 750 mW. The fundamental was

divided into three parts. A major fraction of this light was sent to a single pass through second harmonic generator (SHG) system to generate an efficient 532 nm pump source for pumping the OPAs. In our SHG system, a 5-mm-long, 2-mm-wide, and 1-mm-thick dual-band antireflection-coated periodically poled potassium titanyl phosphate (PPKTP) crystal is used as a nonlinear material. The crystal is set inside a homemade oven, in which the temperature is actively controlled around the temperature for achieving maximum SHG output. An electronic feedback circuit is employed to actively stabilize the temperature fluctuation of crystal to ± 0.01 °C. In particular, about 300 mW of green light was produced when the fundamental input power is about 700 mW. However, in the following experiments, about 100 mW of green light, which is generated at fundamental input power of 250 mW, is employed to pump the two OPAs. This power is strong enough to obtain a significant single-pass parametric gain in our two OPAs. Thanks to high nonlinear coefficient of PPKTP, more than 40% SHG efficiency is obtained.

The nonlinear material for generation of squeezing states in our experiment is a single-mode PPLN waveguide (WG) with a length of 5.0-mm and effective core area of 3 μm $\times 5$ μm. The choice for a single-mode PPLN waveguide has the benefit of the transverse confinement and of the possibility of spatial mode control. In bulk crystals, several problems hamper the available gain [19,27,28]. Two phase quadrature of the signal field experience different spatially dependent gains, leading to the introduction of additional modes along with an accompanying loss of squeezing (the phenomenon of gain-induced diffraction). In a waveguide the transverse profile is determined largely by the step-index changes rather than by nonlinear optical index changes, so the mode can be controlled [29,30]. This leads to more efficient nonlinear interaction between the pump and signal fields and also produces a squeezed field in a well-defined spatial mode. After the generated second harmonic light exited the SHG system, we separate the second harmonic from the fundamental wave. Furthermore, the second harmonic was divided into two beams, which allow pumping the two OPAs systems. The pump lights are carefully focused into the OPAs (WGs) with lenses. The down-conversion signal produced in the OPAs are then collimated with an antireflection-coated lenses and propagates to a 50:50 beam splitter, where they will be spatial and temporal overlap and interference to form the entanglement state. The phase of one of two squeezed vacua is locked so that the squeezing ellipses are perpendicular to each other. Under this condition, the entanglement state is generated which is the quantum resource in quantum information experiments. Each of entangled beams is measured on a homodyne detector by mixing with a LO light.

To observe a high degree of quadrature squeezing and quantum entanglement, we believe that it is very important to achieve a LO which matches the generated squeezed vacuum very well. Contrary to the previous work, in which the remaining 1064 nm light from SHG system is used a LO [19], the LO pulses are obtained by splitting a small portion of the laser emission. Because we found that the temporal envelope of remaining light from SHG is greatly changed from that of the fundamental wave [31]. The intensity and
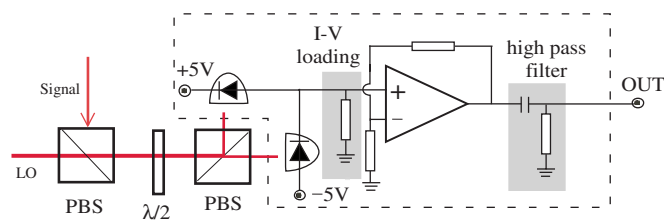
FIG. 2. (Color online) Homodyne system. PBS: polarizing beam splitter, $\lambda/2$: half-wave plate.

polarization of the LO beam are adjusted with a set of half-wave plate and polarizer (not shown in Fig. 1). Then it was passed through a similar PPLN waveguide to ensure proper spatial mode matching to the signal. The LOs and signal (orthogonally polarized to each other) are spatially overlapped at polarizing beam splitter (PBS) and propagate collinearly to a balanced homodyne detector. Before the mixing at PBS, the LO delayed temporally to ensure simultaneous arriving with the signal pulse and the phase of LO can be varied by scanning a prism that is mounted on a piezoelectric translator (PZT).

Another small fraction (about 2 mW) of the fundamental beam is taken out to serve as a probe to study classical parametric amplification occurring in the OPAs. Once again, the probe is also delayed temporally to ensure simultaneous arriving OPA with pump pulses and the phase of probe light relative to the pump light is varied by scanning the prism that is mounted on a PZT.

B. Homodyne detector

Homodyne detector is one of the most important apparatus in quantum optics experiments. It provides a measurement of the field quadratures of signal fields. It consists in mixing the unknown signal field with a strong reference LO field and then detecting proportional photodetectors. A schematic of our homodyne detector is shown in Fig. 2. The LO and signal with orthogonal polarization are mixed at the first PBS and propagate collinearly to the balanced homodyne detector. A half-wave plate ($\lambda/2$) is inserted to rotate the beam polarization to 45° and another PBS splits it into equal two beams. The $\lambda/2$ and PBS construct a 50:50 beam splitter, which is necessary for balanced homodyne detection. The orientation of the $\lambda/2$ is controlled by an extremely high-precision rotational mount. The precise rotation of the $\lambda/2$ is crucial to obtaining a true 50:50 split, which is more important in pulsed homodyne detection [32,33]. The two beams were then focused on a pair of InGaAs photodiodes, which are connected and oppositely biased. The photocurrent difference was loaded on a load resistor and further amplified with gain of about ten times by an operational amplifier (CLC425) in a noninverting configuration. The photocurrents difference produced by the two detectors is proportional to the electric field quadrature selected by varying the relative phase between the LO and the signal field. After passing through a high pass filter, the output signal is analyzed by a spectrum analyzer in the frequency domain or digital scope in the time domain. The quantum efficiency for each photo-
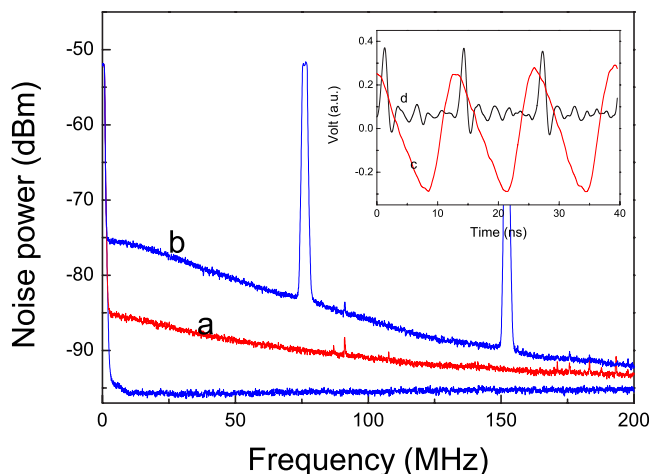

FIG. 3. (Color online) Frequency response of the broadband low noise detector. Trace a: electronical noise, trace b: spectral power of the detected signal when both photodiodes are illuminated by laser pulse with power of 2 mW. Two peaks are due to first and second harmonic frequency of the laser repetition rate. Inset: oscilloscope traces of the homodyne detector at a LO power of 1.5 mW. Trace c: output of homodyne detector, trace d: trigger signal by the Q-switch synchronization from the laser power supply.

diode is measured by comparing the reading of a power meter with mean photocurrent. We obtained $\eta_1 = 0.85 \pm 0.03$ and $\eta_2 = 0.84 \pm 0.03$, respectively.

In order to make high speed op-amp circuit's reliable, stable, low noise and fast, it is necessary to carefully select the electronic components and design the physical layout of the circuit board. Low capacitance photodiode (5 pF) is chosen for getting a wide bandwidth. To keep balance between two sets of homodyne systems for measuring of quantum entanglement, high precision (0.1%) resistors are employed for the load resistor and feedback resistor. For high frequency operation, it is necessary to provide a low impedance path to ground for the bias of photodiode. This is achieved by using a ceramic surface mount chip capacitor (1 μF) and feed through to the ground place. The BNC connector is soldered directly onto the output of op-amp. The photodiode must be placed very close to the op-amp to minimize parasitic capacitance and inductance effect. The two photodiodes were mounted at a distance of as short as possible (1 cm) from each other to minimize spurious rf interferences.

Figure 3 shows a typical frequency spectrum of the detector output at LO power of 2 mW. As can be seen, the detector output has a useful bandwidth to about 200 MHz. The output of homodyne is also measured using a oscilloscope and is shown in the inset of Fig. 3. The output pulses, in which the successive pulses are separated by 13 ns, are clearly distinct from one another. Another key point of our homodyne is its ability to efficiently perform the difference between the intensity fluctuations of the beams impinge on the two detectors. This ability is expressed by the common mode rejection ratio (CMRR) of the balanced detection, defined as ratio between the spectral power measured when both photo detectors (PDs) are illuminated and the spectral power when only one PD is illuminated. We measured it at
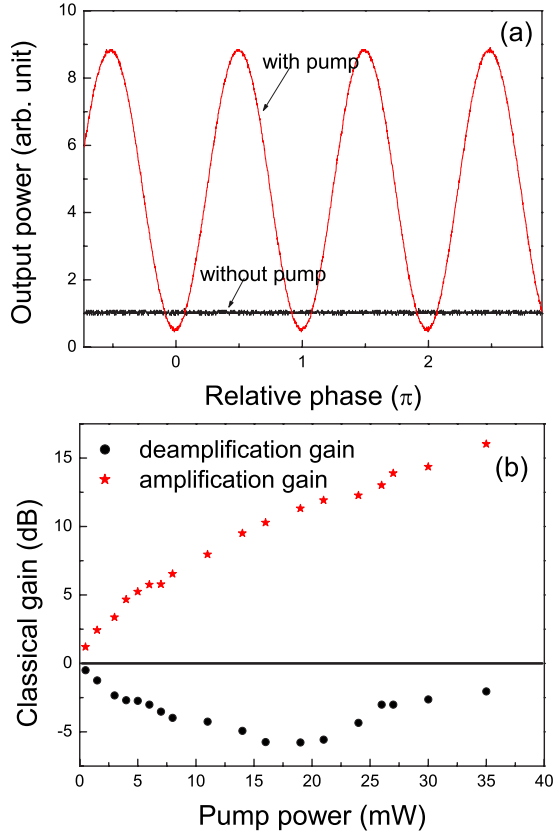
FIG. 4. (Color online) (a) Output probe versus the relative phase between the input probe and pump beams. (b) Classical parametric gain versus average pump power.

the harmonic frequency of the laser repetition rate, obtaining maximum CMRR of 45 dB at low LO laser power and a typical CMRR of more than 20 dB at LO power about of 2 mW, which is the LO power in our measuring of squeezed state and entanglement state. The saturation property of our homodyne is also studied. We found that in the dc signal it does not appear until to LO power of ~10 mW, however the saturation property appears at the LO power of ~4 mW in the rf signal because of the decrease of the CMRR. To prevent the doubtful measurement, we limited the laser power to less than 3 mW in our following measurement.

III. GENERATION OF BROADBAND QUADRATURE SQUEEZING

A. Classical gain

The initial investigation into the characteristics of the OPA is the classical parametric gain. It was measured by introducing a probe light into the OPA. The amplification or deamplification of the input probe signal is observed with an oscilloscope by comparing the output signal power with the pump turned on and off. A typical measurement of phase sensitive amplification of OPA is shown in Fig. 4(a). When the pump is on and the phase of the probe light relative to the pump light is scanned, the output probe signal fluctuates due to the changes of the relative phase. The amplification gain (G_A) and deamplification gain (G_D) is defined as the maxi-

mal probe power and minimum probe power when pump is on divided by probe power when pump is off, respectively. The observed maximum amplification gain and minimum deamplification gain are also shown as a function of the pump average power in Fig 4(b). As shown in figure, a minimum deamplification of −5.7 dB and maximum amplification of 10 dB were obtained at the provided pump power of about 20 mW. With further increase of the pump power, the amplification gain can be monotonously increased; however, the deamplification gain starts to increase instead of to decrease. It seems that the deamplification of the input beam becomes impossible at high pump powers. In the perfect case, the product of amplification gain and deamplification gain should be unity; however the product deviates from unity as the pump power increases as shown in Fig. 4(b). Note the deamplification gain is always less than the amplification gain. Similar disparity between the amplification and deamplification response of an OPA were reported in many experiments on generation of pulsed squeezed state using bulk crystal and the lack of deamplification is due to the phenomenon of gain induced diffraction, which is only occurring at high pump power.

In order to understand the lack of deamplification in the OPA in detail, we established a simple imperfect mode matching model. It is well-known that the lack of deamplification is caused by the distortion of spatial or temporal profile of laser pulse, such as temporal destruction by gain induced diffraction using bulk crystal as nonlinear material, at high pump power. So we can simply assume all the lack of deamplifiction is due to a mis-mode-matching between the pump and probe beams. Taking into account the mode matching efficiency ξ, which means ξ fraction of probe is perfectly overlapped with pump and $1-\xi$ fraction has no overlap, the parametric gain can be written as

$$G_A = \xi \exp(2r) + 1 - \xi,$$

$$G_D = \xi \exp(-2r) + 1 - \xi, \tag{1}$$

where $\exp(2r)$ and $\exp(-2r)$ are the intrinsic parametric amplification gain and deamplification gain and r is the squeezing parameter of OPA system ($r=0$ no squeezing, $r\rightarrow\infty$ ideal squeezing and the ideal limit cannot be achieved experimentally since it requires infinite energy). In reality, the expression should contain a term, which relatives to the pump power; and the general solution of that expression is difficult to obtain [34]. To simplify the expression, we assume that term keeps constant of one under the experimental condition of low pump power (deamplification gain is always less than 1). In this simple model, the squeezing parameter should be proportional to the amplitude of pump field and mode matching efficiency ξ should be constant. The discrepancy of squeezing parameter r and mode matching efficiency ξ indicate the existence of the gain-induced-diffraction- (GID-) like effect. Using this equation, we can estimate squeezing parameter r and mode-matching efficiency ξ from the observed G_A and G_D. The calculated r and ξ versus the pump power are shown in Fig. 5. We can see that squeezing parameter is a nearly linear function of square root of pump power and ξ is almost a constant at low pump power and
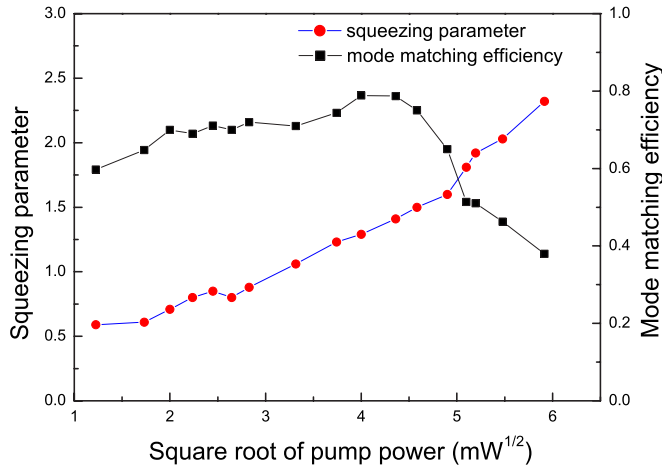
FIG. 5. (Color online) Estimated squeezing parameter and mode matching efficiency versus the square root of the average pump power.

FIG. 6. (Color online) Noise measurement results on a squeezed vacuum generated by a PPLN waveguide. Trace (a) is electronical noise of homodyne detector, trace (b) is shot noise level with LO power of 2.5 mW and trace (c) is the noise power of squeezed vacuum. The two peaks appear at 76 MHz corresponds to the repetition frequency of the mode-locked laser and its second harmonic. Resolution bandwidth is 1 MHz and video bandwidth is 10 Hz.

decreases with the increasing of the pump power at high pump power. In other words, we did not see any evidence of the effect of gain-induced diffraction until the deamplification gain of −5.7 dB (corresponding to pump power of 20 mW). By comparison, a deamplification is about 3 dB when a bulk crystal is exploited in OPA system [19]. At the high pump power, the decreasing of the mode matching efficiency probably caused by the GID-like effect.

B. Measurements of squeezing

The phase sensitive OPA can be exploited for generation of squeezed vacuum state of light. In this run, the OPAs were only pumped by the pump light and the probe signal input was blocked. To measure the squeezing of OPA system, the beam splitter, which is used to interference two squeezed vacua, is removed and the generated squeezed vacua from OPAs are directly mixed with LO beams at PBS and measured by homodyne system, respectively. The output of homodyne detector is recorded using a spectrum analyzer. A typical broadband observation of squeezing is shown in Fig. 6. In this measurement, the analyzing frequency of spectrum analyzer is set from 0 Hz to 200 MHz. At the same time the LO phase is scanned as a parameter; while the frequency is swept, the phase of the LO is advanced independently. We observed the phase sensitive noise with the maximum and minimum corresponding to measurement the antisqueezing and squeezing quadratures, respectively. The shot noise level (SNL) and electronical noise versus frequency are also shown in the figure. The SNL is obtained by blocking the signal input to the homodyne detector and the electronical noise is obtained by blocking both the signal and LO inputs. Noise reduction below the SNL is clearly observed up to 200 MHz. To the best of our knowledge, this is first time noise reduction below SNL has been observed in such a wide bandwidth [18,35].

The squeezing at a fixed analyzing frequency of 10 MHz is shown in Fig. 7. It was obtained by recording the noise power of one homodyne detector with the spectrum analyzer
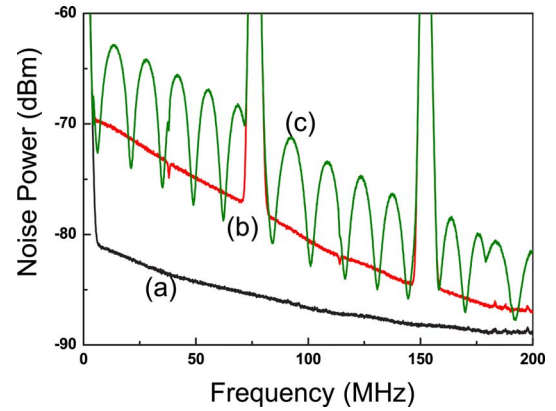
when scanning the phase of the LO. The power of the pump light is fixed at 20 mW. The analyzing frequency of spectrum analyzer is set at center frequency of 10 MHz and span of 0 Hz. The noise level of the vacuum (SNL) is normalized to 0 dB and the electronical noise of homodyne is subtracted. The normalized phase sensitive noise shows 3.4 dB squeezing below the SNL and antisqueezing of 13 dB.

In the absence of perfect detection efficiency, the squeezing is degraded with the overall detection efficiency. Quantum efficiency of photodiode, transmission of optical components, and spatial mode matching can be accounted for by the detection efficiency η_{det}. A further consideration is mismode-matching (ξ) between the probe and pump light because it also introduces noise to the OPA system. So, an overall efficiency η, which is determined by detection efficiency and mode-matching efficiency, is given by $\eta = \eta_{det}\xi$.
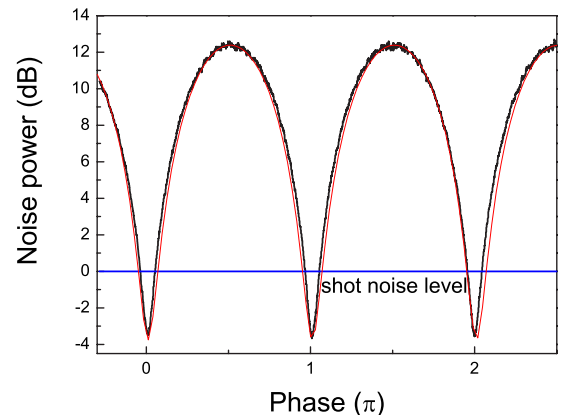

FIG. 7. (Color online) Normalized noise power of squeezed vacuum at fixed analyzer frequency of 10 MHz. The black curve is measured result and the red dashed curve is a fitted result using parameters, which are calculated from the classical amplification and deamplification gain. Resolution bandwidth is 300 kHz and video bandwidth is 100 Hz.
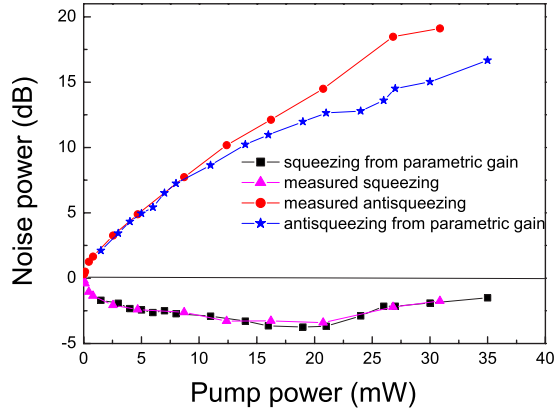
FIG. 8. (Color online) Comparison between the measured normalized noise power of output squeezed state from OPA at different pump power and the predicted noise power from the measured classical gain. The measured noise power were obtained at fixed analyzer frequency of 10 MHz.

A phenomenological expression for the measured noise power can be expressed by

$$P_N(\phi) = \eta[\exp(2r)\cos^2\phi + \exp(-2r)\sin^2\phi] + 1 - \eta, \tag{2}$$

where ϕ is the relative phase of LO. By fitting this formula to the experimental squeezing results we can extract the squeezing parameter r and overall detection efficiency η. The dashed curve in Fig. 7 is a theoretical fit to the data where fitted parameter values are $r = 1.67$ and $\eta = 0.6$. Taking into account of detector quantum efficiency of 0.85, the waveguide loss of 1 dB/cm and the total propagation loss of 3%, we got a total detection efficiency (η_{det}) of 0.71. The fitted value of r and ξ are in good agreement with the estimated values from the parametric gain at a pump power of about 20 mW.

Figure 8 shows the variation of the measured squeezing and antisqueezing with OPA pump power as well as the corresponding theoretical prediction from Eq. (2) based on the measured experimental parameters (amplification gain and deamplification gain) as discussed above. The measured data have been corrected for electronical noise, which is more than 10 dB below the SNL for a LO of about 2 mW. We note that the measured squeezing is in good agreement with the predicted squeezing from amplification gain and deamplification gain parameters. Although the antisqueezing agrees very well with the prediction at low pump power, it is always higher than the prediction at high pump power. This discrepancy might be due to GID-like effect. The calculated squeezing parameter from the amplification gain at high pump power might be less than the squeezing parameter, which is obtained in the experiment. However, the mis-squeezing-parameter does not affect the measured squeezing level, because the squeezing level is mainly dependent on the overall detection efficiency at the high squeezing parameter. From Fig. 8, we note that the squeezing is seen to level off at about 3.0 dB already at a pump of 12 mW while the antisqueezing increases with the pump. It has been demonstrated that the

amount of antisqueezing is also important in practical quantum information experiments. We do our best to increase the amount of the squeezing while at the same point, the antisqueezing has not grown too large. This indicates that in the experiment of generation of entanglement it would be most favorable to operate at this relatively low pump level of OPA to decrease the antisqueezing.

IV. GENERATION AND CHARACTERIZATION OF QUADRATURE ENTANGLEMENT

A. Generation of the entanglement

The scheme, on which the experiment is based, utilizes the superposition of two independently squeezed vacua to create quantum correlations between two output ports. The two output beams a and b have entanglement or EPR correlation of the type originally discussed by Einstein Podolsky, and Rosen. The shadow part in Fig. 1 illustrates this interference and the stick-ball figures graphically show the interference in a phase space representation. The amplitude (X_i) and phase (Y_i) quadrature of the two squeezed vacua at the two input ports are expressed by

$$X_1 = \sqrt{\eta_1}[\exp(-r_1)X_1^{(\text{in})}] + \sqrt{1-\eta_1}X_1^{(v)},$$

$$Y_1 = \sqrt{\eta_1}[\exp(r_1)Y_1^{(\text{in})}] + \sqrt{1-\eta_1}Y_1^{(v)}, \tag{3}$$

$$X_2 = \sqrt{\eta_2}[\exp(-r_2)X_2^{(\text{in})}] + \sqrt{1-\eta_2}X_1^{(v)},$$

$$Y_2 = \sqrt{\eta_2}[\exp(r_2)Y_2^{(\text{in})}] + \sqrt{1-\eta_2}Y_2^{(v)}, \tag{4}$$

the subscript index i ($i=1,2$) indicates the two individual inputs fields and the superscript (in,v) denotes injected vacuum field of the OPAs and vacuum field due to loss, respectively. We assume that both the input vacua and the loss vacuum have the same variance and their variances satisfy the minimum uncertainty states $\langle\Delta^2 X_i^{(\text{in})}\rangle = \langle\Delta^2 Y_i^{(\text{in})}\rangle = \langle\Delta^2 X_i^{(v)}\rangle = \langle\Delta^2 Y_i^{(v)}\rangle = 1/2$. When the squeezing parameter $r_i > 0$, we got the squeezed state with $\langle\Delta^2 X_i\rangle < 1/2$ and $\langle\Delta^2 Y_i\rangle > 1/2$, and the minimum uncertainty state ($\langle\Delta^2 X_i\rangle \times \langle\Delta^2 Y_i\rangle = 1/4$) is destroyed by introducing $0 < \eta < 1$. The quadrature components of the entangled output modes are given in terms of the input squeezed beams and the interference phase θ [36,37]

$$\begin{pmatrix} X_a \\ Y_a \\ X_b \\ Y_b \end{pmatrix} = \begin{pmatrix} t & 0 & -r\cos\theta & r\sin\theta \\ 0 & t & -r\sin\theta & -r\cos\theta \\ r & 0 & t\cos\theta & -t\sin\theta \\ 0 & r & t\sin\theta & t\cos\theta \end{pmatrix} \begin{pmatrix} X_1 \\ Y_1 \\ X_2 \\ Y_2 \end{pmatrix}, \tag{5}$$

where r and t are the amplitude reflection and transmission coefficients of the beam splitter respectively, and they satisfy the relation of $r^2 + t^2 = 1$. The correlation between pairs of quadratures can be readily written as

$$\langle\Delta^2(X_a + X_b)\rangle = (t+r)^2\langle\Delta^2 X_1\rangle + (t-r)^2(\langle\Delta^2 X_2\rangle\cos^2\theta$$
$$+ \langle\Delta^2 Y_2\rangle\sin^2\theta), \tag{6}$$

$$\langle \Delta^2 (Y_a - Y_b) \rangle = (t-r)^2 \langle \Delta^2 Y_1 \rangle + (t+r)^2 (\langle \Delta^2 X_2 \rangle \sin^2 \theta$$
$$+ \langle \Delta^2 Y_2 \rangle \cos^2 \theta). \tag{7}$$

For a particular choice of $r = t = 1/\sqrt{2}$ and $\theta = \pi/2$, the correlation can be rewritten as

$$\langle \Delta^2 (X_a + X_b) \rangle = 2 \langle \Delta^2 X_1 \rangle, \tag{8}$$

$$\langle \Delta^2 (Y_a - Y_b) \rangle = 2 \langle \Delta^2 X_2 \rangle, \tag{9}$$

i.e., they only depend on the squeezing level. For strong squeezed input states ($r_i \to \infty$), perfect quantum correlation $\langle \Delta^2 (X_a - X_b) \rangle \to 0$ and $\langle \Delta^2 (Y_a + Y_b) \rangle \to 0$ are obtained. When we input two coherent states ($r_1 = r_2 = 0$), we get the shot noise level. The SNL in this case is 2 units of vacuum noise, because we are considering the cross correlations between two originally independent fields. However, in a practical case, the interference phase θ is different from $\pi/2$ and the difference between r and t is slightly less or more than zero. In such a case the generated correlation will depend on not only the squeezing level but also the antisqueezing level of the inputted squeezed vacua. Hence, the generated correlation will not have a value as the same value as the inputted squeezing level.

To characterize the entanglement, a well-established approach is to consider the criterion derived by Duan *et al.* [38] and also by Simon [39]. The criterion is based on the total variance of a pair of canonical conjugate variable. It has been demonstrated that, for any separable system, the total variance is bounded from below by a certain value due to the uncertainty relation, whereas for entangled states this bound can be exceeded. The quadratures of electromagnetic fields are a pair of canonical conjugate variable, so the entanglement or equivalently nonseparability can be demonstrated by a violation of the inequality

$$\langle \Delta^2 (X_a + X_b) \rangle + \langle \Delta^2 (Y_a - Y_b) \rangle \ge 2. \tag{10}$$

Entanglement will be present in our system, if both input states are squeezed states ($\langle \Delta^2 X_1 \rangle < 1$ and $\langle \Delta^2 X_2 \rangle < 1$).

B. Measurements of entanglement

There are several ways to witness entanglement. The most intuitive way is to simultaneously measure the correlation of two quantum variables, which have the standard canonical commutation relations, between the two entangled beams. An alternative approach is to construct a quadrature combinations that verify the correlations between original entangled beams by interference the entangled beams on a 50:50 beam splitter [9,40]. The entanglement can be demonstrated by direct detection of the noise variance of quadrature combination of one output only or by measurement the correlation of quadrature combinations between the two outputs. In our experiment, the quality of the entanglement state was investigated both by measuring one entangled beam as well as the correlation between the two entangled beams. The noise in a single entangled beam was measured by fast scanning the local oscillator phase φ of the homodyne detector (200 mHz) while slowly scanning the relative phase θ between the two squeezed vacua (20 mHz). An example is presented in Fig. 9. The observed noise in a single beam of entangled state was obtained by combining two squeezed vacua with squeezing level of 3.2 and 3.0 dB, respectively, while the shot noise level was obtained by blocking the two squeezed vacua inputs. In this run, the rapid sweep of the local oscillator ensures that both quadratures were measured for each value of θ. Hence, the recorded noise of spectrum analyzer can be expressed by
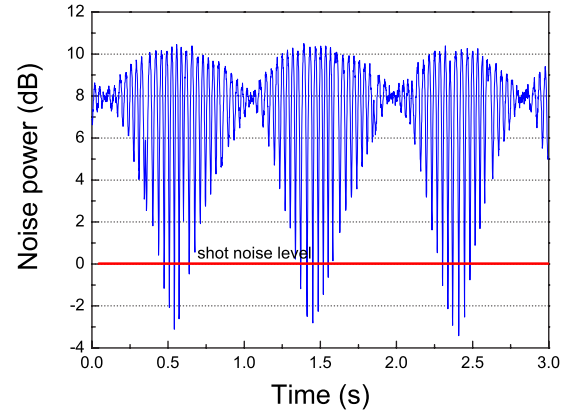

FIG. 9. (Color online) Normalized noise of one beam of the entangled beams obtained by scanning the mutual phase difference between the two squeezed vacua in addition to a rapid sweep of the LO in the homodyne detector.

$$P_N(\varphi) = \cos^2 \varphi \langle \Delta^2 X_a \rangle + \sin^2 \varphi \langle \Delta^2 Y_a \rangle. \tag{11}$$

Without loss of generality, we assume that both squeezed input vacua have the same variances for the squeezed and the antisqueezed quadrature $\langle \Delta^2 X_1 \rangle = \langle \Delta^2 X_2 \rangle = V(\delta_{sq})$ and $\langle \Delta^2 Y_1 \rangle = \langle \Delta^2 Y_2 \rangle = V(\delta_{anti})$. Depending on the relative interference phase θ, the noise powers of $P_N(\varphi)_{\theta=0} = \cos^2 \varphi V(\delta_{sq}) + \sin^2 \varphi V(\delta_{anti})$ at the phase of $\theta = 0$ and $P_N(\varphi)_{\theta=\pi/2} = \frac{1}{2} V(\delta_{anti})$ at the phase of $\theta = \pi/2$ of a single beam can be directly calculated using Eqs. (5) and (11), respectively. As the explained above, the noise of a single beam in Fig. 9 is expected to be phase independent and arises when overlapping two squeezed vacua with a relative phase difference of $\theta = \pi/2$. So, this allows us to identify this point in Fig. 9, and we observed noise power of about 8 dB, which gives noise level of the entangled beam, above the shot noise level. Furthermore, the phase sensitive noise is also observed when the two squeezed vacua are combined in phase ($\theta = 0$). The results shows a noise reduction of about 3 dB, which equals the noise level of squeezed vacuum, below shot noise level and the antisqueezing level of more than 10 dB above the shot noise level. As the expectation, about 3 dB difference between the antisqueezing level and noise level of one entangled beam is observed.

Next, we proceed to the measurement of the entanglement correlation between the two entangled beams via balanced homodyne detection of both of them and subtracting or adding the resulting photocurrents from the two sets of homodyne systems. In this run, the relative phase (θ) of two squeezed vacua was controlled at $\pi/2$ and one of LO phases
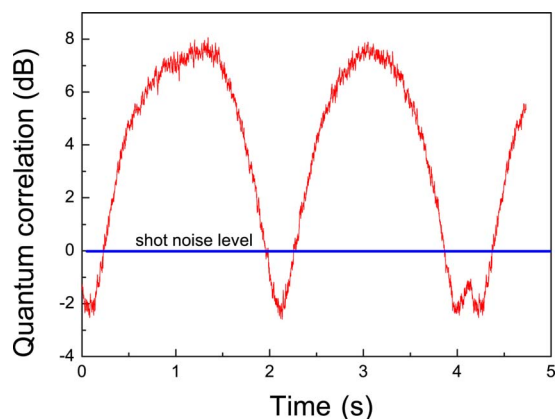
FIG. 10. (Color online) Entanglement correlation between two entangled beams. It is obtained by adding signal of two homodyne detectors measuring the two beams while scanning one of the LO phase.

is fixed on the measurement of one quadrature. The trace in Fig. 10 was a typical recorded noise power spectrum by scanning the LO phase of second homodyne detection and electronically adding the photocurrents of two sets of homodyne detectors. The noise power spectrum was normalized to shot noise level, which was obtained by blocking the squeezed vacua inputs. In such a measurement, the noise power of $X_a + (\sin \varphi X_a + \cos \varphi Y_b)$ was recorded and the noise reduction of about 2.3 ± 0.2 dB below the shot noise level for two beams was observed when the second homodyne detector measure the same quadrature as the first homodyne detector, i.e., $\varphi = \pi/2$. The correlation of another component between two entangled beams can be measured by fixing the LO phase of first homodyne detector to ensure measurement of Y quadrature and electronically subtracting, instead of adding, the photocurrents of two sets of homodyne detectors. In this measurement, the noise power spectrum of $Y_a - (\sin \varphi X_a + \cos \varphi Y_b)$ is given and the noise reduction of

1.6 ± 0.2 dB below shot noise level was obtained when the second LO phase was chosen as $\varphi = 0$.

We translate the aforementioned noise reduction into correlation variance and obtain $\langle \Delta^2(X_a + X_b) \rangle = 0.59 \pm 0.02$ and $\langle \Delta^2(Y_a - Y_b) \rangle = 0.69 \pm 0.02$. The measured values for the correlation variance are plugged into Eq. (10)

$$\langle \Delta^2(X_a + X_b) \rangle + \langle \Delta^2(Y_a - Y_b) \rangle = 1.28 \pm 0.03 < 2, \quad (12)$$

a clear violation of the inequality (10). This result attests for the quantum entanglement of the pulsed state generated by combing two squeezed vacua on a beam splitter. The asymmetry between the correlation measurements between two components mainly due to the phase fluctuation on the beam splitter for the entanglement generation. As discussed in Eqs. (6) and (7), one of components $(Y_a - Y_b)$ is sensitive to the relative phase θ since the drift from $\pi/2$ will introduce the antisqueezing noise to the system.

V. CONCLUSION

In conclusion, we have observed pulsed squeezing and parametric amplification in a PPLN waveguide by use of a cw ML laser. The dependence of the parametric gain on the pump power can be explained by imperfect matching between the pump and the probe beams. Noise reduction below the SNL was clearly observed over a detection bandwidth from near dc to 200 MHz. Direct detection of more than 3.4 dB of squeezing has been achieved in a simple system. The measured squeezing agrees the prediction from parametric gain very well. By combining two squeezed vacua on a beam splitter, the pulsed entanglement state was obtained.

[1] S. L. Braunstein and P. van Loock, Rev. Mod. Phys. **77**, 513 (2005).

[2] *The Physics of Quantum Information*, edited by D. Bouwmeester, A. K. Ekert, and A. Zeilinger (Springer, Berlin, 2000).

[3] *Quantum Information with Continuous Variables*, edited by S. Braunstein and A. K. Pati (Kluwer Akademic Press, Dordrecht, 2003).

[4] A. Furusawa, J. Sørensen, S. L. Braunstein, C. A. Fuchs, H. J. Kimble, and E. Polzik, Science **282**, 706 (1998).

[5] X. Y. Li, Q. Pan, J. T. Jing, J. Zhang, C. D. Xie, and K. C. Peng, Phys. Rev. Lett. **88**, 047904 (2002).

[6] Z. Y. Ou, S. F. Pereira, H. J. Kimble, and K. C. Peng, Phys. Rev. Lett. **68**, 3663 (1992).

[7] Z. Y. Ou, S. F. Pereira, and H. J. Kimble, Appl. Phys. B **55**, 265 (1992).

[8] Y. Zhang, H. Wang, X. Y. Li, J. T. Jing, C. D. Xie, and K. C. Peng, Phys. Rev. A **62**, 023813 (2000).

[9] J. Wenger, A. Ourjoumtsev, R. Tualle-Brouri, and P. Grangier, Eur. Phys. J. D **32**, 391 (2005).

[10] J. Laurat, T. Coudreau, G. Keller, N. Treps, and C. Fabre, Phys. Rev. A **70**, 042315 (2004).

[11] A. S. Villar, L. S. Cruz, K. N. Cassemiro, M. Martinelli, and P. Nussenzveig, Phys. Rev. Lett. **95**, 243603 (2006).

[12] J. T. Jing, S. Feng, R. Bloomer, and O. Pfister, Phys. Rev. A **74**, 041804(R) (2006).

[13] T. C. Zhang, K. W. Goh, C. W. Chou, P. Lodahl, and H. J. Kimble, Phys. Rev. A **67**, 033802 (2003).

[14] W. P. Bowen, R. Schnabel, P. L. Lam, and T. C. Ralph, Phys. Rev. Lett. **90**, 043601 (2004).

[15] V. Josse, A. Dantan, A. Bramati, M. Pinard, and E. Giacobino, Phys. Rev. Lett. **92**, 123601 (2004).

[16] C. Silberhorn, P. K. Lam, O. Weiß, F. König, N. Korolkova, and G. Leuchs, Phys. Rev. Lett. **86**, 4267 (2001).

[17] O. Glöckl, U. L. Andersen, and G. Leuchs, Phys. Rev. A **73**, 012306 (2006).

[18] T. Hirano and M. Matsuoka, Opt. Lett. **20**, 1153 (1992).

[19] T. Hirano, K. Kotani, T. Ishibashi, S. Okude, and T. Kuwamoto, Opt. Lett. **30**, 1722 (2005).

[20] K. Schneider, R. Bruckmeier, H. Hansen, S. Schiller, and J. Mlynek, Opt. Lett. **21**, 1396 (1996).

[21] Y. Zhang, K. Hayasaka, and K. Kasai, Opt. Express **14**, 13083 (2006).

[22] A. I. Lvovsky, H. Hansen, T. Aichele, O. Benson, J. Mlynek, and S. Schiller, Phys. Rev. Lett. **87**, 050402 (2001).

[23] A. Ourjoumtsev, R. Tualle-Brouri, and P. Grangier, Phys. Rev. Lett. **96**, 213601 (2006).

[24] A. Zavatta, S. Viciani, and M. Bellini, Science **306**, 660 (2003).

[25] A. Ourjoumtsev, R. Tualle-Brouri, J. Laurat, and P. Grangier, Science **312**, 83 (2006).

[26] J. Wenger, R. Tualle-Brouri, and P. Grangier, Phys. Rev. Lett. **92**, 153601 (2004).

[27] C. Kim and P. Kumar, Phys. Rev. Lett. **73**, 1605 (1994).

[28] S. K. Choi, R. D. Li, and P. Kumar, J. Opt. Soc. Am. B **17**, 1564 (1997).

[29] M. E. Anderson, D. F. McAliser, M. G. Raymer, and M. C. Gupta, J. Opt. Soc. Am. B **14**, 3180 (1997).

[30] Y. Eto, T. Tajima, Y. Zhang, and T. Hirano, Opt. Lett. **32**, 1698 (2007).

[31] Y. Eto, T. Tajima, Y. Zhang, and T. Hirano, Jpn. J. Appl. Phys., Part 2 **45**, L821 (2006).

[32] H. Hansen, T. Aichele, C. Hettich, P. Lodahl, A. I. Lvovsky, J. Mlynek, and S. Schiller, Opt. Lett. **26**, 1714 (2001).

[33] A. Zavatta, M. Bellini, P. L. Ramazza, F. Marin, and F. T. Arecchi, J. Opt. Soc. Am. B **19**, 1189 (2002).

[34] C. Kim, R. D. Li, and P. Kumar, Opt. Lett. **19**, 132 (1994).

[35] K. Yoshino, T. Aoki, and A. Furusawa, Appl. Phys. Lett. **90**, 041111 (2007).

[36] G. Leuchs, T. C. Ralph, Ch. Silberhorn, and N. Korolkova, J. Mod. Opt. **46**, 1927 (1999).

[37] N. Korolkova, Ch. Silberborn, O. Glöckl, S. Lorenz, Ch. Marquardt, and G. Leuchs, Eur. Phys. J. D **18**, 229 (2002).

[38] L. M. Duan, G. Giedke, J. I. Cirac, and P. Zoller, Phys. Rev. Lett. **84**, 2722 (2000).

[39] R. Simon, Phys. Rev. Lett. **84**, 2726 (2000).

[40] J. Mizuno, K. Wakui, A. Furusawa, and M. Sasaki, Phys. Rev. A **71**, 012304 (2005).